Comparison of Water Vapor Data at the Southern Great Plains Site and its Implications for Water Vapor Continuum Absorption in the Near-Infrared During the ARM Enhanced Shortwave Experiment Period

A. M. Vogelmann, V. Ramanathan and W. C. Conant
Center for Atmospheric Sciences and Center for Clouds, Chemistry and Climate
Scripps Institution of Oceanography
La Jolla, California

Introduction

Several studies find that the observed atmospheric solar absorption is systematically greater than that computed by models in clear skies (Wild et al. 1995; Charlock and Alberta 1996; Arking 1996; Kato et al. submitted). Arking (1996) estimates this excess absorption to be 25 to 30 Wm^{-2} (diurnal and global average) and to be correlated with water vapor amount and uncorrelated with cloud amount. This implies that model treatments of water vapor absorption may be inadequate or that models do not account for absorbers that correlate with water vapor.

Uncertainties that exist in modeling water vapor absorption include the line parameter values and the treatment of the water vapor continuum. Unlike longwave models, shortwave models typically do not include a continuum, and its omission would cause an underestimation of the water vapor absorption. Furthermore, a review by O'Neill et al. (1993) suggests that the magnitude of the continuum has significant uncertainties, with near-infrared continuum absorption coefficients from various studies differing from one another by an order of magnitude. Such uncertainties have likely been narrowed as a result of better and more rigorous theoretical treatments (e.g., Clough et al. 1989; Ma and Tipping, 1992); however, such efforts have focused primarily on the longwave. Further, direct, high-resolution measurements of the continuum at near infrared wavelengths are scarce.

Our objectives are to 1) explore the magnitude of continuum absorption at near-infrared wavelengths by comparing model calculations of water vapor transmission with those observed during the ARM Enhanced Shortwave Experiment (ARESE) period and 2) to assess whether including a near-infrared continuum in model calculations can explain a significant amount of the clear sky excess absorption.

ARESE Data and Modeling

Narrowband water vapor transmission and aerosol optical depths are retrieved from direct beam irradiances measured by the Multifilter Rotating Shadow-band Radiometer (MFRSR) (Harrison et al. 1994). Data are used from the two independent MFRSRs located at the central facility: one that is part of SIROS and the other from the BSRN. The MFRSR has six narrow bands (0.01 μm wide) centered at 0.415, 0.5, 0.61, 0.665, 0.862, and 0.94 μm. The 0.94 μm of the MFRSR (channel 6) is centered on a moderately strong water vapor absorption band. The MFRSR calibration accuracy is estimated to be 5% (J. Michalsky, personal communication) with a reproducibility of -1%.

Cloud-free ARESE days are selected by verifying that the visible direct beam MFRSR irradiances change smoothly with solar zenith angle for the day and that the morning and afternoon values are approximately the same for equal solar zenith angles. Eleven ARESE days are determined as being cloud-free; with the 20-second measurement frequency, this yields over 16,000 measurements with which to conduct this study.

For these days, the transmission by water vapor is retrieved from the direct beam irradiances in the 0.94-μm channel by removing the contributions by Rayleigh and aerosol extinction. The Rayleigh extinction is removed by using Rayleigh calculations from sonde data, and the aerosol optical depth in channel 6 is taken to be equal to that determined for the nearby window channel 5 (0.862 μm). Equating the aerosol optical depth in channel 6 to that in 5 is justified by analyses that find equivalent results when other channels and procedures are used (details in Conant et al., submitted; Vogelmann et al., submitted).

These clear air water vapor transmissions are compared with those computed by state-of-the-art line-by-line and correlated-k models. The original versions of these algorithms were provided by W. Ridgway of Applied Research Corporation working at the Goddard Space Flight Center of the National Aeronautic and Space Administration. The line-by-line model treats the centers of the line profiles as Voigt; the far line wings may be treated as Lorentzian or be replaced by the super-Lorentzian far wing continuum by Clough et al. (1989; hereafter referred to as the CKD continuum). The continuum model version used is CKD_2.2. The line-by-line model was validated by the very close agreement found in comparisons made with Line-By-Line Radiative Transfer Model (LBLRTM) calculations (described in Clough and Iacono, 1995). The line-by-line model inputs water vapor profiles from balloon soundings and computes a set of correlated-k values for each profile.

For the 11 clear sky ARESE days, there are 40 daytime sondes from which correlated-k coefficients are computed for the 0.94-µm band, subdivided into 100 sub-bands. Calculations with the correlated-k coefficients agree to within 0.6% with the line-by-line calculations from which they were constructed; so any significant differences between the calculations and the observations is due to the physics in the line-by-line model, not the correlated-k representation thereof. The 0.94-µm direct beam irradiances are computed for every 20-second interval using the water vapor column measured by the microwave radiometer (MWR) and the vertical distribution and correlated-k coefficients from the nearest sonde launch (in time).

The MWR data from the ARM archive have been reprocessed as advised by the instrument mentor (J. Liljegren, personal communication) to remove the tuning function. Thus, in the special case of the ARESE period, the coincident, independent measures of column water vapor by the sondes and the MWR show excellent agreement with a mean bias of 1% and a rms difference of 5% (Figure l). We note that this level of sonde-MWR agreement is rather atypical and that much larger differences exist at other times, indicating the need and importance for studies such as those conducted during the Water Vapor IOP.

Results

We compare the modeled and observed water vapor transmission, respectively $\langle T_{H20}\rangle_{MODEL}$ and $\langle T_{H20\ DATA}\rangle$, through the following least squares regression

$$-\ln\langle T_{H20}\rangle_{MODEL} = A_0 + A_1(-\ln\langle T_{H20}\rangle_{DATA})$$

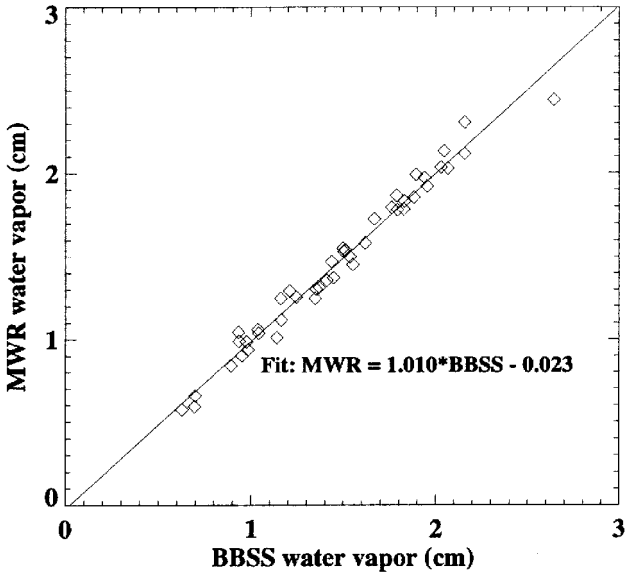

Figure 1. Microwave radiometer (MWR) comparison to sondes. Column-integrated water vapor amounts from the MWR and sondes from the balloon-borne sounding system (BBSS) are compared for clear-sky days during ARESE. The least squares regression plotted gives the average relationship between the BBSS and the MWR column water vapor.

where A_0 and A_1 are determined by the regression. A_0, the bias or offset, results from potential error sources including the instrument calibration offset and any bias errors in the model physics. We use $-\ln\langle T_{H2O}\rangle$ in this regression, rather than $\langle T_{H2O}\rangle$, so that any potential errors in transmission that are unrelated to the trending with water vapor loading (e.g., instrumental offset errors) will be separated in the A_0 term. For example, the contribution of the 5% in instrument calibration uncertainty to A_0 is $0.05A_1$. A_1 quantifies how well the model can represent the rate at which the atmospheric transmission decreases with an increase in the water vapor path. If theory and observations match exactly, $A_0 = 0$ and $A_1 = 1$. An error analysis of the sensitivity of A_0 and A_1 is given in Conant et al. (submitted), which estimates the uncertainty in this regression technique to be ±0.02 in A_0 and ±0.02 in A_1.

Many shortwave models assume the line shape to be Lorentzian. Thus, for reference, we first compare the SIROS data with model calculations that treat the far wings as Lorentzian (Figure 2). Close agreement is found: the bias is within the $0.05A_1$ uncertainty from the instrument calibration, A_1 indicates a 5% model underestimation of the observed trend in $-\ln\langle T_{H2O}\rangle_{DATA}$ with water vapor path. Similar results are found when the BSRN data are used. For a rigorous

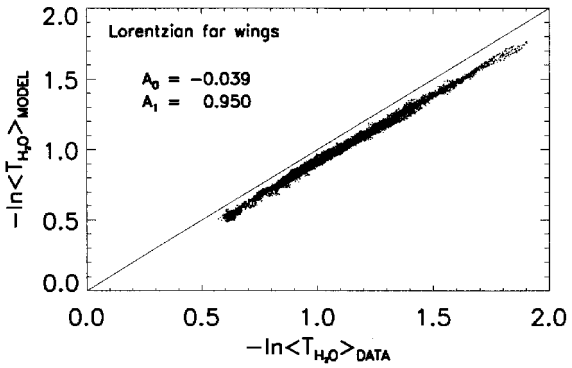

Figure 2. Lorentzian far wing comparison. Comparison between $-\ln\langle T_{H2O}\rangle_{DATA}$ and the $-\ln\langle T_{H2O}\rangle_{MODEL}$ computed with the correlated-k distributions that use a Voigt profile with Lorentzian far wings.

discussion of this analysis and its broadband energetic consequences, see Conant et al. (submitted). Because A_1 is less than unity, more water vapor absorption is needed for the model to agree with the observed trend in $-\ln\langle T_{H20}\rangle_{DATA}$.

We next regress the observations to the model calculations that include the CKD continuum (Figure 3). The extreme sensitivity of this regression method is illustrated by noting that the addition of the continuum, which is orders of magnitude less than the strong line optical depths in the 0.94-μm region, results in such a dramatic change in the regression. The slope (A_1) has increased from 0.95 to almost 1.10, and

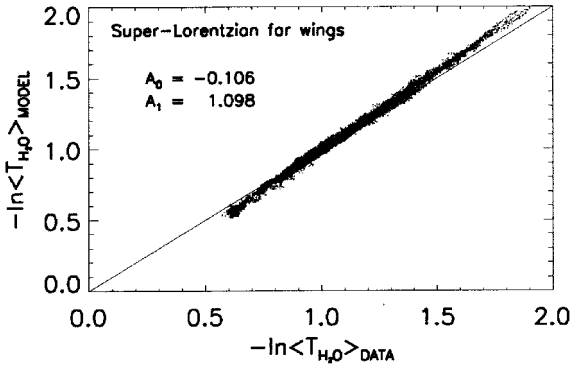

Figure 3. Continuum (super-Lorentzian) comparison. Comparison between $-\ln\langle T_{H20}\rangle_{DATA}$ and the $-\ln\langle T_{H20}\rangle_{MODEL}$ computed with the correlated-k distributions that use a Voigt profile with the CKD_2.2 Continuum.

the bias (A_0) has tripled to exceed the uncertainty from instrument calibration by a factor of two. Thus the model calculations, which are based on the current state of knowledge of the line parameters and water vapor amounts, indicate that the dependence of transmission in this band with the water vapor path is too great. A full error analysis will be conducted on the sensitivity of this result to uncertainties, including those in the line parameters, water vapor profiles, and continuum magnitude.

Finally, because shortwave models typically neglect the continuum at near infrared wavelengths, we assess the broadband impact of this assumption. We compute the downward solar irradiances at the surface (from 0.5 to 3.5 μm) treating the far wings as Lorentzian and with the CKD continuum; the difference between these calculations is the additional solar absorption effected by the continuum. Diurnal averages of the atmospheric absorption are computed by a δ4-stream-discrete-ordinates-method algorithm that includes Rayleigh scattering and water vapor absorption computed using the correlated-k model. Four clear-sky profiles are chosen to represent a range of column water vapor amounts found in our climate, and the solar geometry used produces a daylight-average solar zenith angle of 53°. The results (Table 1) indicate that the continuum enhances atmospheric absorption by 1 to 2 Wm^{-2} for a diurnal average and 4 to 6 Wm^{-2} for noontime. Thus, it is unlikely that significant amounts of clear sky excess absorption on the order of 15 to 30 Wm^{-2} (diurnally averaged) can be explained by the continuum.

Table 1. Additional atmospheric continuum broadband solar absorption. Atmospheric absorption is computed for the spectral region from 0.5 to 3.5 μm, with the far line wings modeled as Lorentzian and replaced by the CKD continuum model; the difference between these calculations is the additional broadband absorption effected by the continuum (tabulated). Lorentzian wings are truncated ±300 cm^{-1} from line center.

Profile	Water vapor column (cm)	Additional continuum absorption (Wm^{-2})	
		24-hr Avg.	Noon
ARESE			
Minimum	0.69	1.5	3.9
Median	1.34	1.7	4.4
Maximum	2.04	1.9	4.8
CEPEX	3.94	2.3	5.9

Conclusions and Future Research

We have shown that observations support the existence of a continuum in the 0.94-µm band, which would contribute more absorption than a standard Lorentzian model. The model calculations that invoke the CKD continuum overestimate the absorption in this region, which could be due to uncertainties including those in the line parameters, water vapor amounts or magnitude of the continuum. Further studies are planned to address the sensitivity of these results to such uncertainties. Regardless, broadband calculations (0.5 to 3.5 µm) indicate that replacing the Lorentzian far wings (typically assumed in shortwave models) with the CKD continuum can enhance atmospheric absorption by up to 2 Wm^{-2} (diurnal average). Thus, it is unlikely that inclusion of the continuum can account for a significant fraction of the clear sky excess absorption on the order of 25 to 30 Wm^{-2}.

Acknowledgments

We thank the ARM SGP and ARM ARESE teams for access to and interpretation of the data. We thank J. Michalsky and J. Barnard for discussions about the MFRSR, J. Liljegren for discussion about the MWR, and W. Ridgway for providing the original versions of the line-by-line and correlated-k algorithms used. We are grateful to S. A. Clough and Eli Mlawer for their critical feedback on this work and discussions about the CKD continuum. This work was supported by Department of Energy Atmospheric Radiation Measurement program grant DE-FG03-9lER61198.

References

Arking, A., 1996: Absorption of solar energy in the atmosphere: Discrepancy between model and observations, *Science*, **273**, 779-782.

Charlock, T. P., and T. L. Alberta, 1996: The CERES/ARM/GEWEX Experiment (CAGEX) for the retrieval of radiative fluxes with satellite data, *Bull. Amer. Meteor. Soc.*, **77**, 2673-2683.

Clough, S. A., and M. J. Iacono, 1995: Line-by-line calculation of atmospheric fluxes and cooling rates. 2. Application to carbon dioxide, ozone, methane, nitrous oxide and the halocarbons, *J. Geophys. Res.*, **100**, 16519-16535.

Clough, S. A., F. X. Kneizys, and R. W. Davies, 1989: Line shape and the water vapor continuum, *Atmos. Res.*, **23**, 229-241.

Conant, W. C., A. M. Vogelmann, and V. Ramanathan. The unexplained solar absorption and atmospheric water vapor: A test with Tropical Pacific and ARM-ARESE Oklahoma data, *Science* (submitted).

Harrison., L. C., J. J. Michalsky, and J. Berndt, 1994: Automated multifilter rotating shadow-band radiometer: an instrument for optical depth and radiation measurements, *Appl. Opt.*, **33**, 5118-5125.

Kato, S., T. P. Ackerman, E. E. Clothiaux, J. H. Mather, G. G. Mace, M. L. Wesely, F. Murcray, and J. Michalsky. Uncertainties in modeled and measured clear-sky surface shortwave irradiances, *J. Geophys. Res.* (submitted).

Ma, Q., and R. H. Tipping, 1992: A far wing line shape theory and its application to the foreign broadened water continuum absorption. III, *J. Chem. Phys.*, **97**, 2, 818-828.

O'Neill, N. T., A. Royer, P. Cote, and L.J.B. McArthur, 1993: Relations between optically derived aerosol parameters, humidity, and air-quality data in an urban atmosphere, *J. Appl. Meteor.*, **32**, 1484-1498.

Vogelmann, A. M., V. Ramanathan, W. C. Conant, and W. E. Hunter. Observational Constraints on Non-Lorentzian Continuum Effects in the NearInfrared Solar Spectrum Using ARM ARESE Data, J. *Quant. Spectrosc. Radiat. Transfer* (submitted).

Wild, M., A. Ohmura, H. Gilgen, and E. Roeckner, 1995: Validation of general circulation model radiative fluxes using surface observations, *J. Climate*, **8**, 1309-1324.